

Journal of Biomedical Optics

BiomedicalOptics.SPIEDigitalLibrary.org

Early detection of virus infection in live human cells using Raman spectroscopy

Kamila Moor
Yusuke Terada
Akinori Taketani
Hiroko Matsuyoshi
Kiyoshi Ohtani
Hidetoshi Sato

SPIE.

Kamila Moor, Yusuke Terada, Akinori Taketani, Hiroko Matsuyoshi, Kiyoshi Ohtani, Hidetoshi Sato, "Early detection of virus infection in live human cells using Raman spectroscopy," *J. Biomed. Opt.* **23**(9), 097001 (2018), doi: 10.1117/1.JBO.23.9.097001.

Early detection of virus infection in live human cells using Raman spectroscopy

Kamila Moor, Yusuke Terada, Akinori Taketani, Hiroko Matsuyoshi, Kiyoshi Ohtani, and Hidetoshi Sato*
Kwansei Gakuin University, School of Science and Technology, Department of Biomedical Chemistry, Sanda, Hyogo, Japan

Abstract. Virus infection of a human cell was determined only 3 h after invagination. We used viral vector Ad-CMV-control (AdC), which lacks the *E1* gene coding for early polypeptide 1 (E1). AdC can replicate in human embryonic kidney 293 (HEK293) cells into which the *E1* gene has been transfected. According to partial least-square regression discriminant analysis, it was assumed that two kinds of reaction take place in the cell during viral invasion. The first response of the cell was determined 3 h after the virus invasion, and the second one was determined ~9 h later. The first one seems to be due to compositional changes in DNA. Analysis of large-scale datasets strongly indicated that the second reaction can be attributed to a reduction in protein concentration or uptake of phenylalanine into the nucleus. © 2018 Society of Photo-Optical Instrumentation Engineers (SPIE) [DOI: 10.1117/1.JBO.23.9.097001]

Keywords: Raman spectroscopy; virus; infection.

Paper 180140R received Mar. 20, 2018; accepted for publication Aug. 6, 2018; published online Sep. 4, 2018.

1 Introduction

Raman spectroscopy has advantages for biomedical applications because it can be used to noninvasively examine a single live cell without labeling. In our previous study, virus infection was successfully detected in individual live human cells by Raman spectroscopy within 12 h after addition of a virus into the culture medium.¹ We used a recombinant adenovirus, Ad-CMV-control (AdC), which lacks genes *E1* and *E3*, and HEK293 cells that possess the *E1* gene. The *E1* gene contains the promoter of the *E2* gene. *E2* codes for a DNA polymerase that is specific to replication of the viral genome. These genes coding early proteins are localized to the nucleus. The *E3* gene is related to suppression of the immune system. The lack of this gene has no effect on the cultured cells used in this study. Therefore, AdC can infect and replicate in HEK293 cells. This technique has several advantages over conventional immunostaining and genetic tests for detection of human infectious viruses. It does not require any genetic or proteomic information about the virus in advance. Because it detects spectral changes in a live cell that are caused by virus infection, it is possible to monitor the virus invasion over long periods. These advantages suggest that the proposed technique is suitable for detection of human infectious viruses in many environments. Salman et al.² applied Raman spectroscopy for identification of the infection of Vero cells by herpes simplex virus of type 1 (HSV1) and 2 (HSV2) and by varicella zoster virus. They proposed to identify virus types at 24 h after infection. This approach shows good suitability of Raman spectroscopy for virus detection and identification, but at the same time, implies a challenging question regarding the origin of a difference in Raman spectra.

Development of a practical monitoring method for viral pathogens is important not only for prevention of a pandemic, such as pandemic of Ebola hemorrhagic fever, but also for early detection of oncogenic viral infections. By the modern

diagnostic methods, it is possible to detect the presence of a human infectious virus only when the symptoms appear in the infected people, e.g., a cough and fever. These symptoms may manifest themselves too late for prevention of fatal effects of the infection. The mainstream methods for diagnosis are based on the detection of viral antigens and/or nucleic acids of viruses, but they generally require specialized equipment and trained personnel. To reduce the costs and time, some emerging diagnostic assays have been developed, such as a proximity ligation assay, biosensor-based methods, fluorescence resonance energy transfer-based methods, microarray assays, and in particular, nanoparticle-based techniques.³ Nevertheless, identification of the virus type in advance is necessary for an assay even by these new methods because they are based on molecular biology. Silva et al.⁴ studied the metabolism of HEK293 and 1G3 cells (an amniocyte-derived cell line) associated with adenovirus infection. They observed specific uptake and secretion rates of metabolites during the virus infection by ¹H nuclear magnetic resonance spectroscopy. According to their results, HEK293 and 1G3 cells show significant differences in metabolite consumption even in response to infection by the same adenovirus. This finding indicates that the cellular response totally depends on the cell type, even though the products are synthesized by the same virus. Tip-enhanced Raman spectroscopy and surface-enhanced Raman spectroscopy are also applied to virus detection and identification.⁵⁻⁷

The purpose of this study is to develop a technique for detection of virus infection within a short period by Raman spectroscopy and to investigate the origin of the spectral changes. Raman spectroscopy is a powerful tool for studying reactions in intact live cells.⁸⁻¹² The Raman analysis proposed here offers an opportunity to detect unknown human infectious viruses in the absence of human patients. It works on cultured human cells and indicates the presence of a virus within a short period. In this study, we investigate what kind of alteration Raman analysis detects during invasion of a virus. There are two possible

*Address all correspondence to: Hidetoshi Sato, E-mail: hidesato@kwansei.ac.jp

reactions taking place in the infected cell: one is the fast reaction attributed to the response of the cell to viral invasion, and the other is much slower and involves duplication of the virus. The first reaction includes transfer of the virus into a lysosome, proteolysis, and antigen presentation. The second one includes expression of early genes and production of capsid proteins. To study the mechanism of the viral propagation, time-lapse Raman observation was conducted for 24 hours. The spectral changes were studied in more detail in comparison with our previous research. This study may improve the methodology of virus research. Because Raman analysis can detect virus infection in a single cell, the experiment can be conducted with fewer virus particles than the minimal accessible number of virus particles during a clinical infection. Hence, this study is important for evaluation and estimation of the feasibility of Raman spectroscopy for virus studies.

2 Experimental Setup

HEK293 cells were purchased from DS Pharma Biomedical (Japan). The cells were cultured in high-glucose Dulbecco's modified Eagle's medium (Wako, Japan) supplemented with 10% of fetal bovine serum (Beit HAEMEK, Ltd., Israel) and 100 IU/mL penicillin (Wako). The cells were cultured in a CO₂ incubator, SCA/SMA-163 (Astec, US), at 37°C and 5% of CO₂. A special dish with a quartz window at the bottom was purchased from Synapse-Gibko (Japan) and used for Raman analyses. A stock of an adenovirus, AdC, was prepared by the method reported in another paper.¹³ The virus was stored at -80°C until experiments. The two virus stocks were used at the viral titer of 0.5×10^6 plaque-forming units/mL. HEK293 cells were checked for mycoplasma infection with a polymerase chain reaction detection kit (e-Myco VALiD, Cosmo Bio, Japan), and the result was negative.

2.1 Immunostaining

The infection by AdC was confirmed by indirect immunofluorescent labeling. The cells were cultured for 0, 3, 12, 24, and 48 h and were stained after the Raman spectroscopy. After careful removal of the medium, the cells were fixed with paraformaldehyde (4%) for 10 min. After two washes with phosphate buffered saline (PBS) without divalent cations [PBS(-)], the fixed cells were incubated with methanol (90%) for 2 min to permeabilize the plasma membrane, then washed thrice with PBS(-). The samples were incubated with antibody to a 72 K viral product (1:1000) diluted in bovine serum albumin with sodium azide, at 36.6°C for 45 min. After incubation with the primary antibody, the samples were washed thrice with PBS(-) for 5 min each. The samples were incubated with a secondary antibody at 36.6°C for 45 min, followed by washing thrice with PBS(-). The secondary antibody, antirabbit IgG antibody, conjugated to Alexa Fluor 546 dye was used for the observation of the samples at 0 and 3 h and that conjugated to fluorescein isothiocyanate (FITC) dye was done for those at 12, 24, and 48 h. Fluorescent images were captured using an A1 confocal fluorescence microscope (Nikon, Tokyo, Japan).

2.2 Raman Spectroscopy

Two Raman microscopes were used in this study. They were both equipped with a CO₂ incubator that maintained the culture dishes at 37°C in an atmosphere containing 5% of CO₂ during the measurements. One of them, Nanofinder

(Tokyo Instruments, Japan), is equipped with an upright microscope. Its water-immersion objective lens (NA = 1.10, Olympus, Japan) was dipped into the culture medium to record the cell spectra. A continuous-wave background-free electronically tuned Ti:sapphire laser (CW-BF-ETL; Mega Opto, Japan) provided an excitation beam at 785 nm. The laser power was typically set to 30 mW during sampling. The exposure time was 90 s (30 s × 3 times). The microscope was equipped with a 60× water-immersion objective lens (NA = 1.10, Olympus, Japan) and a Raman polychromator, which has a grating (600 l/mm, 750 nm-blazed) and a Peltier-cooled CCD detector (DU-401-BR-DD, Andor Technology, Ireland). The spectral resolution was 5 cm⁻¹. This instrument was easy to focus on the sample and was used to record as many spectra as possible within a short period. The analyses were performed at 12, 24, and 48 h after addition of the virus to the cells. The experiments were repeated 5 to 20 times, and all the data were analyzed together.

The other Raman system was constructed in-house and involved an inverted fluorescence microscope. It was utilized for time-lapse experiments because it could keep cells for more than 24 h under the cultivation conditions. The excitation light at 785 nm was provided by a diode laser (Toptica, Germany). The laser power was typically set to 50 mW during sampling. The exposure time was 90 s (30 s × 3 times). The microscope was equipped with a 60× water-immersion objective lens (NA = 1.10, Olympus, Japan), a Raman polychromator equipped with a grating (600 l/mm, 750 nm-blazed; Photon Design, Japan) and a Peltier-cooled CCD detector (DU-401-BR-DD, Andor Technology, Ireland). Given that the incubator has two places to set dishes (with control and virus-infected cells), the control and experimental dishes were maintained under the same stable conditions during the analysis. The time-lapse analysis was repeated three times, and the results were very similar.

To acquire the spectra, the laser was focused onto the nuclei of cells. The spectra were recorded in randomly selected cells in each dish. The spectrum of each cell was processed by background subtraction and sixth polynomial fitting to remove the artifacts caused by the culture medium and by the dish window. The intensities of the spectra were normalized to the band at 1004 cm⁻¹, assigned to phenylalanine residues. The spectra were also normalized to a band at 1440 cm⁻¹, assigned to a CH deformation mode, to confirm the results of multivariate analysis. The results obtained for the datasets normalized to the 1440 cm⁻¹ band were always similar to those obtained for the datasets normalized to the 1004 cm⁻¹ band. This finding suggested that the normalization procedures were valid. Multivariate-analysis software, Unscrambler (CAMO, Norway), was used for principal component analysis (PCA) and partial least-square regression discriminant analysis (PLSR-DA). For the PLSR-DA, a dependent variable, -1 or 1, was included in the dataset to classify each dataset.

3 Results and Discussions

The AdC viruses are recombinant adenoviruses capable of invading human cells by similar mechanisms. Given that AdC lacks the *E1* gene, it cannot replicate in a normal human cell. However, it is able to do so in an HEK293 cell that has the *E1* gene after transfection. *E1* protein regulates the *E2* gene, which encodes a DNA polymerase for replication of the viral genome. Figure 1 shows immunostaining images of HEK293

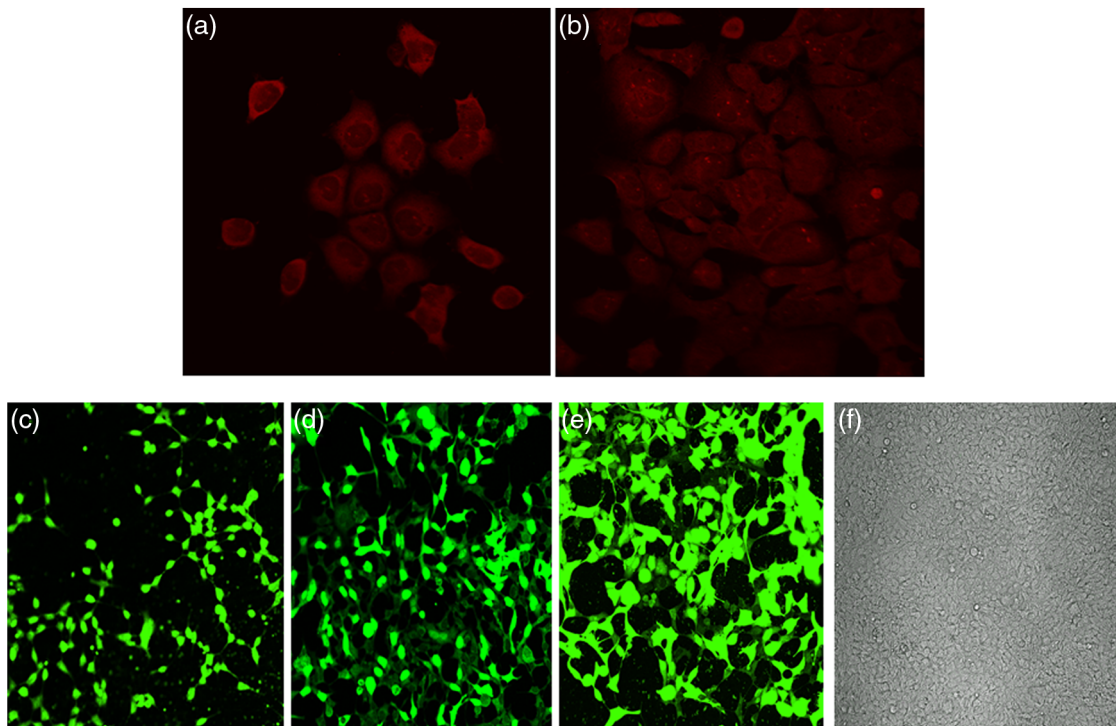


Fig. 1 Immunostaining images of HEK293 cells infected with the AdC virus, observed at (a) 0 h, (b) 3 h, (c) 12 h, (d) 24 h, and (e) 48 h after addition of the virus to the culture medium, and a bright-field image is also shown in (f). The cells were stained with a secondary antibody with (a and b) Alexa Fluor 546 dye and that with (c–e) FITC dye.

cells infected with virus AdC (panels a to e). The antibody to the E2 polypeptide was applied to staining. In our previous paper, nuclei of virus-infected cells at 24 h showed strong fluorescence.¹ In contrast, the entire cell body showed fluorescence in this study because methanol staining here destroyed the nuclear membrane. Since the samples at 0 and 3 h labeled with the secondary antibody with FITC had showed no signal at the first experiment, they were, then, labeled with the secondary antibody with Alexa, which has stronger fluorescent signal. (The filter set and light source were suitable for Alexa dye in our confocal fluorescent microscope.) Their images are shown in Figs. 1(a) and 1(b). They similarly show only faint signals in the images, which are, however, due to nonspecific adsorption, indicating absence of the E2 polypeptide at 3 h after the infection. In contrast, the image at 12 h [Fig. 1(c)] already indicated the presence of the E2 polypeptide, suggesting that the E2 gene was transferred into the nucleus quickly after the virus invasion. The image in Fig. 1(c) shows that ~40% of the cells expressed the E2 polypeptide at 12 h, and the infection rate was almost 60% to 85% for the cells at 24 (d) and 48 h (e). This finding indicates that the rate of infection was high but not in all cells, and the concentration of the E2 polypeptide was low in the sample at 12 h and continuously increased within the cell for up to 48 h.

The averaged Raman spectra of the cells with AdC (a and b) and without the virus (c and d), acquired at 12 and 24 h, are presented in Fig. 2. The spectra are so close to each other that it is difficult to find a difference. Bands at 1655 and 1448 cm^{-1} were assigned to amide I and CH bending modes of proteins, respectively. A sharp band at 1004 cm^{-1} and a minor band at 1030 cm^{-1} were attributed to phenylalanine residues in the proteins. Smaller features at 1337, 1089, and 783 cm^{-1}

attribute to adenine, PO_2^- symmetric stretch, and OPO symmetric stretch modes of DNA, respectively.^{14,15} The observed spectra are similar to those reported in our previous paper.¹ Figure 3 shows PCA analysis results for the datasets obtained in the time-lapse analysis of AdC-infected and control cells. We employed the Raman system with the inverted microscope, and spectra

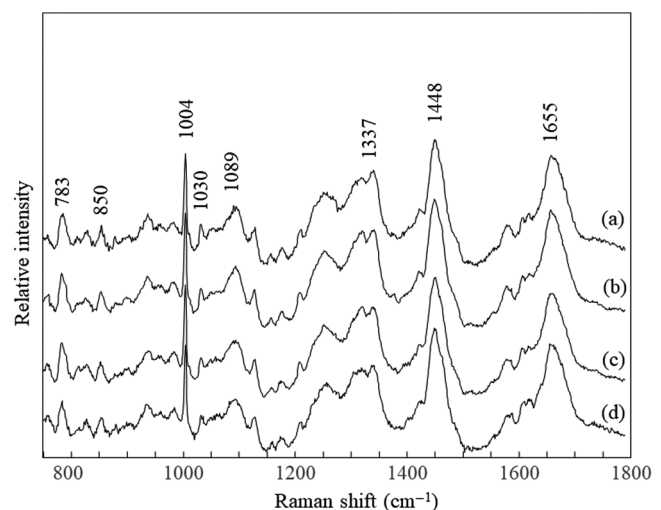


Fig. 2 Averaged Raman spectra of HEK293 cells (a and b) infected with the AdC virus or (c and d) not infected with the virus obtained at 12 and 24 h after addition of the virus, respectively. The measurements were carried out with the confocal Raman system with an upright microscope. (Exposure time: 90 s and excitation light: 785 nm, 30 mW.)

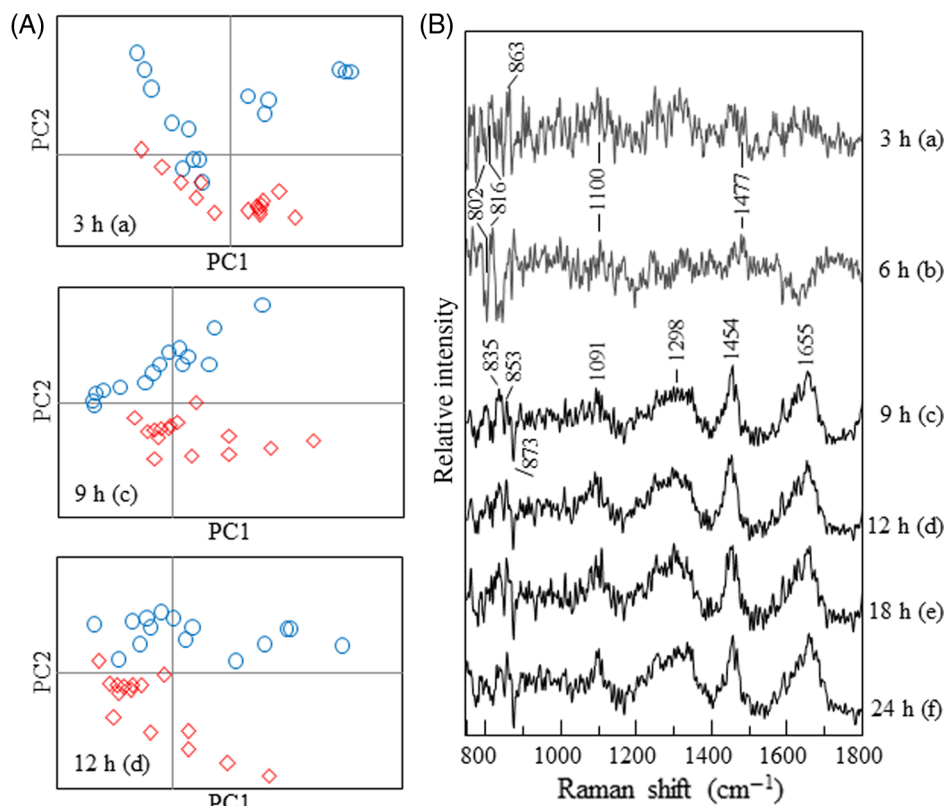


Fig. 3 The PCA score plots for (A) PC1 and PC2 and (B) their PC2 loading plots for the datasets of control cells (○) and AdC virus-infected cells (◊). Results for datasets recorded at (a) 3 h, (b) 6 h, (c) 9 h, (d) 12 h, (e) 18 h, and (f) 24 h after addition of the virus. (Some of score plots are exhibited in the [Appendix](#).)

were repeatedly and alternately acquired from two culture dishes containing the infected and control cells placed in the CO_2 incubator on the microscope stage. The Raman analyses were carried out at 3, 6, 9, 12, 18, and 24 h after the virus injection under the stable cultivation conditions. It took 2 to 3 min for focusing on the nucleus and acquisition of the spectrum at each measuring site. To keep the synchronism in the dataset, the sample measurement was finished in 40 min at each dataset. Therefore, each dataset has relatively small number, 10 to 15, of spectra. The PCA score plots of the datasets acquired at 3 (a), 9 (c), and 12 h (d) are shown in Fig. 3(A). (Those of the datasets recorded at 6, 18, and 24 h are shown in the [Appendix](#)) The score plot at 3 h (a) suggests that the Raman analysis already detected the virus infection at 3 h. The dispersion of data groups, however, overlaps, indicating that the virus invasion process is still under way in several cells. The score plot of the dataset recorded at 6 h (see the [Appendix](#) figure) also shows an overlap of the two groups. The score plots at 9 and 12 h revealed that the datasets of virus-infected cells are well discriminated from the datasets of uninfected control cells. Because it seemed that principal component (PC) 2 made a strong contribution to separation of these two data groups, the loading plot of PC2 represents the major difference in the spectra between the cells with and without virus infection. A similar tendency was observed for other data groups acquired at 6 and 18 h, but PC1 made an equally large contribution in comparison with PC2 for separation of the two data groups in the score plot at 24 h (see the [Appendix](#)). The loading plots of PC2 for datasets recorded at 3 (a), 6 (b), 9 (c), 12 (d),

18 (e), and 24 h (f) are presented in Fig. 3(B). At a glance, a remarkable difference is noticeable between the loading plots at 6 and 9 h. These data indicate that the reaction of the infected cell changed after 6 h. According to the spectral features in the loading plot at 3 and 6 h, the spectral difference between AdC-infected and control cells seems to be attributable to composition changes in DNA and RNA. DNA has a strong and broad band near 790 cm^{-1} and broad-shoulder bands near 830 cm^{-1} , which consist of overlapping small bands. RNA has a band near 783 cm^{-1} and a similar shoulder band. DNA also has strong bands near 1092 and 1488 cm^{-1} . We assumed that the narrow sharp bands in positive and negative directions between 800 and 870 cm^{-1} in the loading plot at 3 and 6 h were generated by a wavenumber shift of the small bands constituting the broad bands derived from DNA and RNA. Small bands at 1100 and 1477 cm^{-1} are also assignable to DNA. The results agree with that of immunostaining observation in Fig. 1. In contrast, the loading plot of PC2 for 9- (c), 12- (d), 18- (e), and 24-h datasets (f) shows protein-like features. This result indicates that the composition of protein species suddenly changed and/or phenylalanine concentration increased in the nucleus of the virus-infected cells. (This is because a band of phenylalanine serves for intensity correction.) This finding suggests that transcription was activated, and the main process for translation of early proteins was moved out of the nucleus.

According to the time-lapse data, we hypothesized that there are two major postinfection reactions inside the cell after entry of the virus. One is the response of the cell itself (Rsp A). The

reaction of the cell is partly known and includes antigen presentation and upregulation of lysosomes.¹⁶ We assumed that this kind of reaction proceeds quickly after addition of the virus and is maintained consistently thereafter because the reaction must be faster than virus propagation to protect cells from the viral invasion. The other is production of early viral polypeptides and proteins to assemble viral particles (Rsp B). This kind of reaction proceeds gradually because the replication of DNA and synthesis of proteins consume a large amount of energy and materials. If these two reactions occurred during the virus infection process in cells, the effect of Rsp A would emerge several hours earlier than that of Rsp B. The Rsp A reaction at an early time point is probably difficult to detect by conventional methods because it does not involve production of proteins or nucleic acid replication in the first several hours. Because the cell must immediately react to the virus invasion, the reaction may activate certain functions and can result in localized molecular composition changes. The Rsp B reaction can be observed by conventional methods, as depicted in the fluorescent images in Fig. 1.

To analyze the origin of spectral changes in detail and to improve the reliability of the analysis, it is necessary to increase the number of data points in the datasets. The number of data points was relatively small in our previous study.¹ The time-lapse analysis is a time-consuming process, and it is not possible to increase the number of data points within the limited period. There is another problem: background subtraction in the spectral processing for the time-lapse experiments. Because there was no time to acquire the background spectrum after the recording of each dataset, background spectra of the medium and dish were collected after the time-lapse examination. The same background data were shared to process all the data obtained in one experiment. Strictly speaking, this procedure should normally be avoided because there are differences in consumption and secretion of materials in a culture medium between the control and infected cells.¹⁷ Therefore, we could not rule out that

the present time-lapse data may be affected by the background spectra. Hence, we repeated the whole experiment many times to collect as much data as possible. In these experiments, the Raman system with an upright microscope was used, and the samples were prepared in a conventional CO₂ incubator. With the upright microscope, it was easy to find a target cell, but the water-immersion objective lens that was inserted into the culture dish may cause contamination of the cell culture. The background measurements were carried out in every culture dish and were discarded after each Raman spectroscopy session. To keep uniformity of data and to minimize the time-dependent changes, the analysis was carried out only within 1 h in each culture dish where only 10 to 15 cells were analyzed. For technical reasons, it was difficult to conduct measurements earlier than 12 h after the infection.

We obtained several dozen sample spectra as well as background spectra in the experiments independently repeated via the same procedure for further analysis. The datasets were subjected to PCA at first. In the PCA results of time-lapse spectra (Fig. 3), the spectral alterations due to virus infection were seen in the earliest components, such as PC1 and PC2, which reflect the largest dispersion in the datasets. In contrast, PCs from 1 to 7 yielded no remarkable categorization among these datasets, suggesting that they reflect spectral changes caused by cell conditions, such as slight differences due to cultivation conditions among the repeated experiments as well as inherent activities. We assumed that there were large irregular variations that were not related to the virus infection in this large set of data. The cell and virus are sensitive to alterations in the experimental conditions, such as concentrations of ingredients in the culture medium and conditions of storage, which technically cannot be eliminated. When the spectral changes due to the viral infection are smaller than those due to irregular variations, it is difficult to find them in the earlier components in PCA. Hence, PLSR-DA was applied to extract variations that strongly correlated with the independent variable.¹⁸

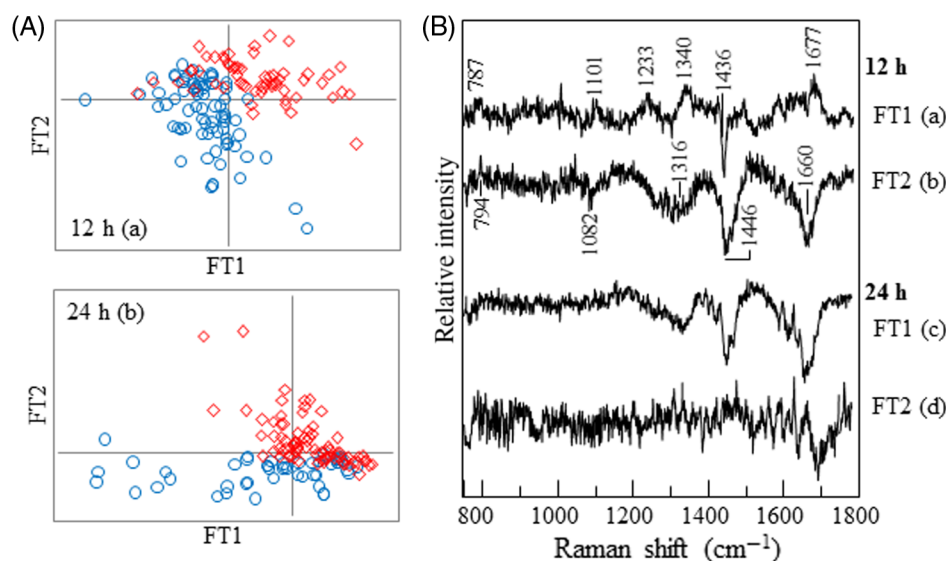


Fig. 4 PLSR-DA results obtained for control cells (○) and AdC virus-infected cells (◇). (A) Score plots for FT1 and FT2 calculated from the datasets obtained at 12 h (a, control: $n = 73$; AdC: $n = 59$) and 24 h (b, control: $n = 48$; AdC: $n = 78$) after addition of the virus to the cells. (B) Loading plots of (a) FT1 and (b) FT2 for the datasets acquired at 12 h, and (c) FT1 and (d) FT2 for the datasets recorded at 24 h.

In the PLSR-DA, two datasets were analyzed together, where “-1” and “1” are tags for the independent variables. Therefore, a factor (FT) obtained by PLSR-DA was selected to make the dispersions of the two data groups distant, thus representing a characteristic difference between these data groups. Score plots for FT1 and FT2 are shown in Fig. 4(A) for the datasets of control cells and AdC-infected cells analyzed at 12 (a) and 24 h (b) after addition of the virus, respectively. The dispersion in the dataset of the cells with a virus partly overlaps with that of the control cells. Several spectra of the infected cells are present in the control group, suggesting that the nonspecific spectral variance was quite strong and/or some cells were not infected by the virus yet as suggested by the immunostaining. The PLSR-DA model was validated by the one-leave-out cross-validation method. The correlation coefficient values (R^2) of the PLSR-DA models built for four FTs were 0.842 and 0.665 for validation results of datasets acquired at 12 and 24 h, respectively. Loading plots of FT1 and FT2 for the models of 12- and 24-h datasets are shown in Fig. 4(B). The loading plots of FT2 for the 12-h dataset (b) and of FT1 for the 24-h dataset (c) look like that of PC2 [Fig. 3(B) (d)] in the time-lapse experiment in the high-frequency region. The positive and negative directions are opposite because the direction of distribution in FT2 is opposite in the score plots [Figs. 3(A) (d) and 4(A) (a)]. Bands at 1660 and 1436 cm^{-1} and broad features near 1340 cm^{-1} can be attributed to a protein. The negative direction of these bands indicates downregulation of proteins relative to the phenylalanine concentration or the uptake of phenylalanine into the nucleus, because of the virus infection. However, the spectral features are slightly different in the low-frequency region. Bands at 787 and 794 cm^{-1} may be assigned to differential bands between

DNA and RNA molecules. In case of plants, the response to pathogens would be accompanied by biosynthesis of aromatic compounds involving the conversion of phenylalanine.¹⁹ However, any cellular response involving phenylalanine has not been reported for mammal cells, as far as we know. The present results suggest that Raman spectroscopy can detect virus infection in a live cell *in vitro*, even in its dormant state or during slow replication. This approach has advantages over the conventional methods, which require expression of viral genes.

4 Conclusion

Raman spectroscopy can detect the infection with adenovirus in a single live human cell without staining or labeling within only 3 h after addition of the virus to the culture medium. The analysis with a large number of datasets confirms that an HEK293 cell shows specific reactions to the virus infection. The present results suggest that there are two kinds of reactions taking place in the cell under the influence of virus infection. The first kind occurs instantly after the virus invasion. The second kind of reaction seems to represent viral gene expression and replication of the virus particles. It seems to include uptake of phenylalanine into the nucleus and/or excess protein production.

Appendix

Figure 5 shows the PCA score plots for PC1 and PC2 for the datasets of control cells (blue, circle) and AdC virus-infected cells (red, diamond), recorded at (a) 3 h, (b) 6 h, (c) 9 h, (d) 12 h, (e) 18 h, and (f) 24 h after addition of the virus.

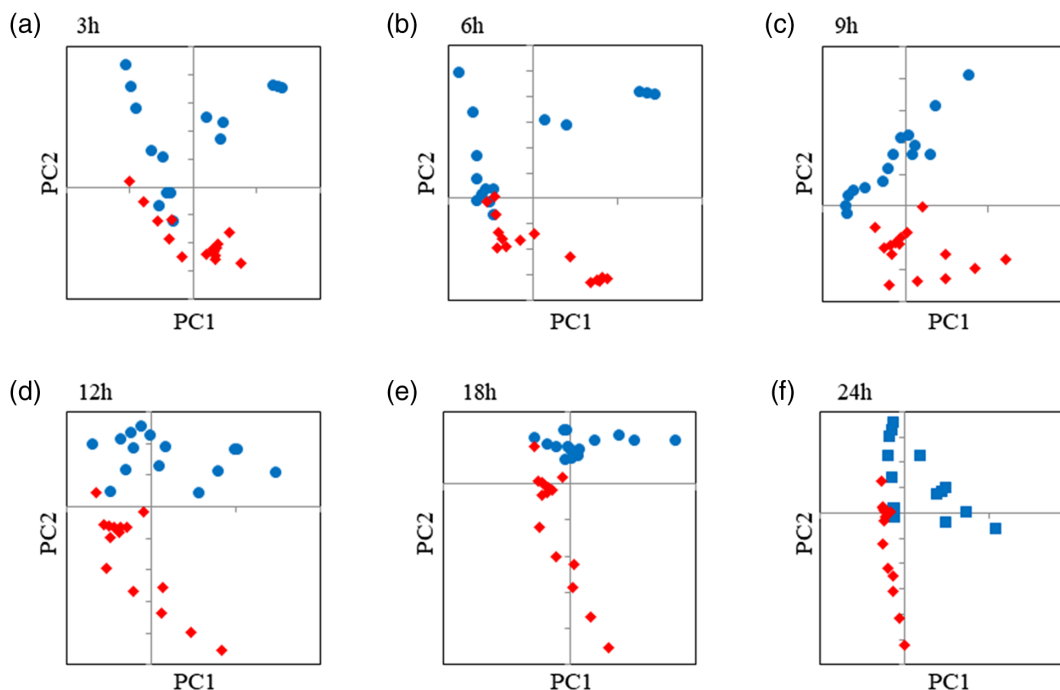


Fig. 5 The PCA score plots for PC1 and PC2 for the datasets of control cells (blue, circle) and AdC virus-infected cells (red, diamond), recorded at (a) 3 h, (b) 6 h, (c) 9 h, (d) 12 h, (e) 18 h, and (f) 24 h after addition of the virus.

Disclosures

The authors have no relevant financial interests in this article and no potential conflicts of interest to disclose.

Acknowledgments

This study was supported by the Japan Society for the Promotion of Science KAKENHI under the Grant No. 25560211.

References

1. K. Moor et al., "Noninvasive and label-free determination of virus cells by Raman spectroscopy," *J. Biomed. Opt.* **19**(6), 067003 (2014).
2. A. Salman et al., "Characterization and detection of Vero cells infected with Herpes Simplex Virus type 1 using Raman spectroscopy and advanced statistical," *Methods* **68**, 364–370 (2014).
3. G. Glockzin et al., "Characterization of the recombinant adenovirus vector AdYB-1: implications for oncolytic vector development," *J. Virol.* **80**, 3904–3911 (2006).
4. A. C. Silva, A. P. Teixeira, and P. M. Alves, "Impact of adenovirus infection in host cell metabolism evaluated by ¹H-NMR spectroscopy," *J. Biotechnol.* **231**, 16–23 (2016).
5. D. Cialla et al., "Raman to the limit: tip-enhanced Raman spectroscopic investigations of a single tobacco mosaic virus," *J. Raman Spectrosc.* **40**, 240–243 (2009).
6. J. Lim et al., "Identification of newly emerging influenza viruses by surface-enhanced Raman spectroscopy," *Anal. Chem.* **87**, 11652–11659 (2015).
7. V. Hoang et al., "Identification of individual genotypes of measles virus using surface enhanced Raman spectroscopy," *J. Analyst* **135**, 3103–3109 (2010).
8. K. Hamada et al., "Raman microscopy for dynamic molecular imaging of living cells," *J. Biomed. Opt.* **13**, 044027 (2008).
9. G. J. Puppels et al., "Studying single living cells and chromosomes by confocal Raman microspectroscopy," *Nature* **347**, 301–303 (1990).
10. I. W. Schie and T. Huser, "Methods and application of Raman microscopy to single-cell analysis," *J. Appl. Spectrosc.* **67**, 813–828 (2013).
11. J. R. Nottingher et al., "Application of FTIR and Raman spectroscopy to characterization of bioactive materials and living cells," *Spectroscopy* **17**, 275–288 (2003).
12. K. Hartmann et al., "A study of Docetaxel-induced effects in MCF-7 cells by means Raman microspectroscopy," *J. Anal. Bioanal. Chem.* **403**, 745–753 (2012).
13. K. Ohtani et al., "Regulation of cell growth-dependent expression of mammalian CDC6 gene by the cell cycle transcription factor E2F," *J. Oncogene* **17**, 1777–1785 (1998).
14. S. C. Erfurth, E. J. Kiser, and W. L. Peticolas, "Determination of the backbone structure of nucleic acids and nucleic acid oligomers by laser Raman scattering," *Proc. Nat. Acad. Sci. U. S. A.* **69**, 938–941 (1972).
15. J. M. Benevides and G. J. Thomas Jr., "Characterization of DNA structures by Raman spectroscopy: high-salt and low-salt forms of double helical poly(dG-dC) in H₂O and D₂O solutions and application to B, Z and A-DNA," *Nucleic Acids Res.* **11**, 5747–5761 (1983).
16. J. E. Teigler, J. C. Kagan, and D. H. Barouch, "Late endosomal trafficking of alternative serotype adenovirus vaccine vectors augments antiviral innate immunity," *J. Virol.* **88**, 10354–10363 (2014).
17. T. R. Shojaei et al., "A review on emerging diagnostic assay for viral detection: the case of avian influenza virus," *Mol. Biol. Rep.* **42**, 187–199 (2015).
18. K. A. Lê Cao, S. Boitard, and P. Besse, "Sparse PLS discriminant analysis: biologically relevant feature selection and graphical displays for multiclass problems," *BMC Bioinf.* **12**, 2–16 (2011).
19. J. F. Bol, H. J. M. Linthorst, and B. J. C. Cornelissen, "Plant pathogenesis-related proteins induced by virus infection," *Annu. Rev. Phytopathol.* **28**, 113–138 (1990).

Kamila Moor received her bachelor's degree in the Microbiological Department and master's degree in the Chemistry Department of Kazakhstan National University, Al-Farabi. Currently, she conducts her research for a doctor degree at the Graduate School of Science and Technology, Kwansei Gakuin University, Japan. She also has a researcher position in chemistry laboratory at Nazarbaev University, Kazakhstan.

Biographies for the other authors are not available.